Nucleic Acids Research, 1998, Vol. 26, No. 11 **2665–2671**

Triple helices containing arabinonucleotides in the third (Hoogsteen) strand: effects of inverted stereochemistry at the 2′-position of the sugar moiety+

Anne Noronha and Masad J. Damha*

Department of Chemistry, McGill University, 801 Sherbrooke Street West, Montreal H3A 2K6, Canada

Received February 10, 1998; Revised and Accepted April 8, 1998

ABSTRACT

Arabinonucleic acid, the 2′-stereoisomer of RNA, was tested for its ability to recognize double-helical DNA, double-helical RNA and RNA–DNA hybrids. A pyrimidine oligoarabinonucleotide (ANA) was shown to form triple-helical complexes only with duplex DNA and hybrid DNA (Pu):RNA (Py) with an affinity that was slightly lower relative to the corresponding pyrimidine oligodeoxynucleotide (DNA) third strand. Neither the ANA nor DNA third strands were able to bind to duplex RNA or hybrid RNA (Pu):DNA (Py). In contrast, an RNA third strand recognized all four possible duplexes (DD, DR, RD and RR), as previously demonstrated. Such an understanding can be applied to the design of sequence-selective oligonucleotides which interact with double-stranded nucleic acids and emphasizes the role of the 2′-OH group as a general recognition and binding determinant of RNA.

INTRODUCTION

The past few years have seen an explosive growth in the use of oligonucleotide analogs to target RNA sequences for the treatment of human diseases (the ‘antisense’ approach; 1,2). Undoubtedly, a major factor contributing to these developments is the facility with which synthetic oligonucleotides are available today (3–5). Another area that is receiving significant experimental attention is the regulation of DNA function by triple helix formation (the ‘antigene’ approach; for recent reviews see 6–8). This approach is of considerable interest as triplex formation allows the design of therapeutic agents capable of site-specific inhibition of transcription (9), the development of DNA biosensors (10) and artificial DNA nucleases (11,12) and the detection of mutations within duplex DNA (13).

Triple-helix formation can occur when an oligonucleotide strand (the ‘third strand’) binds in the major groove of the targeted duplex (14–16). Several nucleic acid triple-helices have been characterized, which fall into two distinct classes depending on the sequence and the mode of binding of the third strand to the duplex. In the triplex pattern termed the ‘pyrimidine motif’, a pyrimidine-rich third strand binds parallel to the purine strand of the Watson–Crick duplex. Formation of $T{\cdot}$AT and $C^{+}{\cdot}$GC base triads occurs as a result of Hoogsteen hydrogen bonding interactions between the pyrimidine bases of the third strand (C^{+} and T) and the purine bases of the target duplex. In the alternative ‘purine motif’, the third (purine-rich) strand binds antiparallel to the purine strand of the duplex through the reverse Hoogsteen base pairing scheme (A*AT, G*GC and T*AT triplets, where N* indicates the base in the third strand) (6–8).

Several studies have shown that the chemical nature of the sugars has a dramatic influence on the triple-helix (D-ribose versus D-2-deoxyribose) (17–21). Significantly, in the pyrimidine motif, a more stable triplex is formed when the third strand is RNA rather than DNA, with *RNA*·DNA:RNA being among the most stable of the observed triplexes (hereafter RNA and DNA strands are abbreviated to R and D respectively). In addition, a third *R* strand forms a stable triplex with all duplex combinations, i.e. DD, DR, RD and RR, whereas a third *D* strand forms a stable triplex only with DD and DR duplexes (D being a purine-rich strand). The structural basis for these effects is unknown. Possible explanations include hydrogen bonding interactions between the 2′-OH groups in the third strand and the phosphates of the purine strand, hence the stabilization of R·DD triplexes compared with D·DD (19). However, it has been shown that methylation of the 2′-OH groups in the third strand leads to even further stabilization of the triplexes formed, probably due to hydrophobic effects (24). In contrast to the general accommodation of RNA strands in the pyrimidine triplex motif, a stable triplex forms in the purine triplex motif only when *all* three of the component strands are DNA (22,23).

Our laboratory has recently focused upon the synthesis of arabinonucleic acids (ANA), a stereoisomer of RNA based on D-arabinose instead of the natural D-ribose (Fig. 1). In an earlier study, we synthesized a series of oligoarabinose homopolymers and demonstrated that (araAp)$_7$araA forms a complex with poly(rU) having a 2U:1A stoichiometry (25). More recently, we have shown that oligoarabinonucleotides of mixed base composition form Watson–Crick duplexes with complementary DNA and RNA strands (26) and that araC-rich ‘forked’ oligomers associate into C-tetrads (or *i*-motif) structures (27). In the present study we wished to investigate whether the stabilizing effect exerted by

*To whom correspondence should be addressed. Tel: +1 514 398 7552; Fax: +1 514 398 3797; Email: damha@omc.lan.mcgill.ca

+Dedicated to the memory of Professor R. T. Walker

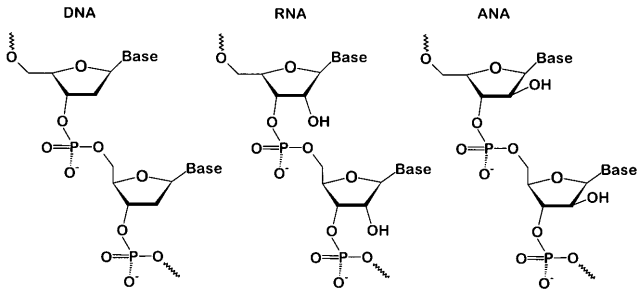

Figure 1. Structure of DNA, RNA and arabinonucleic acids (ANA).

ribose in the pyrimidine triplex motif is also observed for arabinose. Can an oligoarabinonucleotide fit into a duplex major groove and, if so, how is triple-helix stability influenced by the stereochemistry at the 2′ position of the third strand? This knowledge would increase our understanding of the molecular forces that stabilize triple-helices, which, in turn, could allow us to predictably improve binding properties of triplex-forming oligonucleotides. Our results revealed that arabinonucleic acid strands (abbreviated ANA or *A*) form triplexes with DD and DR, but not RD and RR duplexes. The lack of association of *A* strands with duplexes containing oligoribopurines and the fact that *D*→*A* substitution in the third strand has little effect on the thermal stability of triplexes formed suggests that *D* and *A* strands share common conformational characteristics. In addition, these results are consistent with the notion that the 2′-OH in the ribose configuration plays a crucial role in the stabilization of triple-helices.

MATERIALS AND METHODS

Oligonucleotide synthesis

Oligoribonucleotides and oligoarabinonucleotides, whose sequences are shown in Figure 2, were assembled on an Applied Biosystems Model 381A synthesizer using standard cyanoethylphosphoramidite chemistry (4,28). Long chain alkylamine controlled pore glass (CPG), derivatized with araU or riboU monomer (29), was used as the solid support. Prior to chain assembly, the support (1 µmol) was treated with the capping reagents, acetic anhydride, *N*-methylimidazole, 4-dimethylamino pyridine, as previously described (28). Assembly of sequences was carried out as follows. (i) Detritylation: 3% trichloroacetic acid in dichloroethane delivered in 100 s (+ 40 s burst) steps. The eluate from this step was collected and the absorbance at 504 (DMT+, ribo sequences) and 478 nm (MMT+, arabino sequences) measured to determine condensation yields (79–109% for *A* strands). (ii) Nucleoside phosphoramidite coupling for 7.5 min. (iii) Capping: 1:1 (v/v) acetic anhydride/collidine/THF 1:1:8 (solution A) and 1-methyl-1*H*-imidazole/THF 16:84 (solution B) delivered in 62 + 35 s 'wait' steps. (iv) Oxidation: 0.05 M iodine in THF/water/pyridine 7:2:1, delivered in 20 + 35 s 'wait' steps. The 5′-terminal trityl group was removed by the synthesizer and the oligomers were then removed from the support and deprotected by treatment of the CPG with a solution containing concentrated ammonium hydroxide/ethanol (3:1 v/v, 1.2 ml) for 2 days at room temperature. The RNA sequences were further

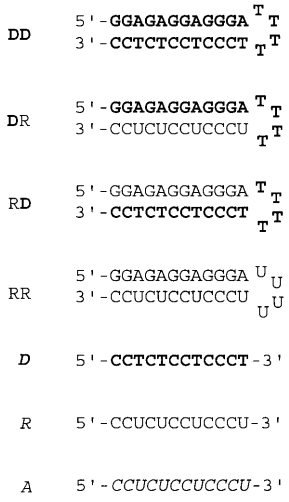

Figure 2. Hairpin duplexes (DD, DR, RD and RR) and single strands (D, R and A) selected for study (17). DNA sequences are shown in bold.

deprotected (2′-desilylation) by treatment with $NEt_3 \cdot 3HF$ (100 µl) at room temperature for 48 h (28). The deprotected oligomers were purified by preparative PAGE followed by gel filtration (desalting) on a Sephadex G-25 column (28). Oligodeoxynucleotides were obtained commercially from the University of Calgary DNA Synthesis Laboratory (Calgary, Alberta, Canada). The mass spectra of the *A* strand was consistent with its assigned structure (calculated mass 3602.4 g/mol, found 3602).

UV thermal denaturation studies

Molar extinction coefficients for oligonucleotides were calculated from those of the mononucleotides and dinucleotides according to nearest-neighbor approximations (30). The values for the hybrid hairpins were assumed to be the sum of their *D* + *R* components: *D*, 9.1; *R*, 9.6; DD, 26.5; DR, 27.1; RD, 26.7; RR, 27.7 (units = 10^4/M/cm). The molar extinction coefficient for the *A* strand was assumed to be the same as the normal *R* strand (9.6×10^4/M/cm). Complexes were prepared by mixing equimolar amounts of interacting strands, e.g. *A* + hairpin DD, and lyophilizing the resulting mixture to dryness. The resulting pellet was then redissolved in a buffer containing 100 mM NaOAc, 1 mM EDTA (pH 5.5). The final concentration was 2 µM in each strand. The solutions were then heated to 80°C for 15 min, cooled slowly to room temperature and stored at 4°C overnight before measurement. Prior to the thermal run, samples were degassed by placing them in a speed-vac concentrator (2 min). Denaturation curves were acquired at 260 nm at a rate of heating of 0.5°C/min, using a Varian CARY Model 1 spectrophotometer fitted with a six sample thermostable cell block and a Peltier temperature controller. The data was analyzed with the software provided by Varian Canada and transferred to Microsoft Excel for presentation. Melting temperatures (T_m) were calculated from the first derivative of the melting curves. Hyperchromicity data (*H* %) are reported as the percent increase in absorbance at the wavelength of interest with respect to the final absorbance in accordance with the convention of Puglisi and Tinoco (30).

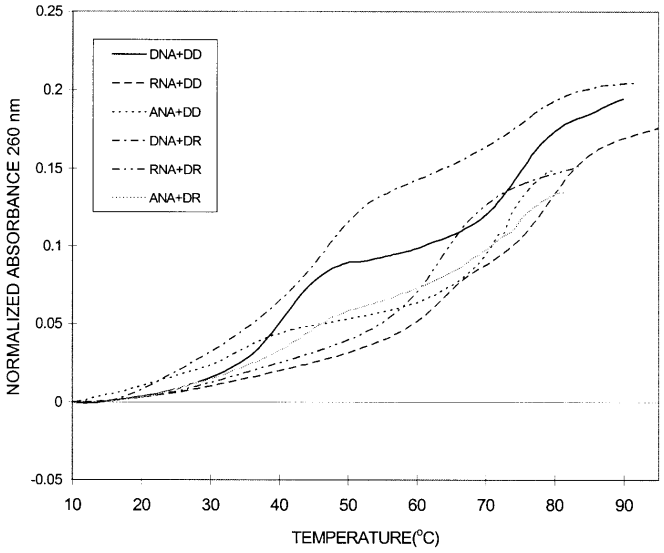

Figure 3. UV melting curves of complexes (2 µM) in 100 mM sodium acetate buffer, 1 mM EDTA (pH 5.5).

Circular dichroism (CD) spectra

CD spectra (200–350 nm) were collected on a Jasco J-710 spectropolarimeter equipped with a constant temperature circulating bath (NESLAB RTE-111). Each spectrum was an average of five scans collected at a rate of 100 nm/min using fused quartz cells (165-QS; Hellma). Measurements were carried out at 5°C in 100 mM NaOAc, 1 mM EDTA buffer (pH 5.5), at a final concentration of 2 µM in each strand (for triplex and duplex melting) and 5 µM (for single strands). The data were processed on a PC computer using Windows-based software supplied by the manufacturer (Jasco Inc.). To facilitate comparisons, molar ellipticities were calculated from the known nucleotide concentrations and the new spectra obtained.

Gel electrophoresis

For native gels (20% polyacrylamide) solutions of oligonucleotides were first lyophilized and incubated in 10 µl 30% sucrose in 1 M NaOAc, 10 mM EDTA buffer (pH 5.0) at 70°C for 15 min. This solution was then cooled to room temperature and finally incubated at 4°C overnight (concentration in each strand 2 µM). The samples were loaded onto the gel, which was run with a buffer containing 100 mM NaOAc, 1 mM EDTA (pH 5.0) at 100 V for 6–8 h. Denaturing gels (14% polyacrylamide, 7 M urea, pH 8) were run as previously described (28). All gels were visualized by UV shadowing (28).

RESULTS

Experimental design

To study the interaction of arabinonucleic acids with duplexes, we adopted the experimental design of Roberts and Crothers, which has been successful in analyzing the effects of DNA and RNA composition of 'pyrimidine motif' triple-helices (17). The target duplexes are Pu/Py hairpins and contain the four possible combinations of DNA and RNA strands (designated DD, DR, RD and RR, where the first letter describes the 5′-homopurine stem strand and the second letter the 3′-homopyrimidine sequence) (Fig. 2). The oligoarabinopyrimidine strand (*A*) illustrated in Figure 2 was synthesized to explore triple-helix formation with the hairpin duplexes. For the purpose of comparison, the known oligoribopyrimidine (*R*) and oligodeoxyribopyrimidine (*D*) sequences were also examined. The ability of these oligomers to form triple-helices was determined from UV spectroscopic melting experiments, native gel electrophoresis and CD spectroscopy, in a solution containing 100 mM sodium acetate and 1 mM EDTA, pH 5.5.

Table 1. Thermal dissociation of complexes in 100 mM sodium acetate, 1 mM EDTA buffer (pH 5.5)

Duplex	Third strand	T_m (°C)	
		First	Second
DD	D	40	75
	R	62	77
	A	34	75
DR	D	45	75
	R		69[a]
	A	43	73
RD	D		84
	R	43	86
	A		84
RR	D		84
	R	45	85
	A		84

Oligonucleotide concentration is 2.0 µM in each strand.
[a]Single transition for triplex→R + hairpin DR→DR (coil) processes (17).

UV melting studies

The results of the melting experiments are shown in Figure 3 and Table 1. Of the four possible triplexes containing *A* as the third strand, only *A*·DD and *A*·DR were observed to form. This was indicated by the presence of two transitions in the absorbance versus temperature profile when solutions containing equal concentrations of each *A* and duplex DD or DR were heated at a rate of 0.5°/min (Fig. 3). The low temperature transition corresponds to dissociation of the arabino strand (*A*) from the target DD and DR duplexes. This assignment is based upon the observation that the low temperature transition disappears at neutral pH, whereas the high temperature transition was essentially independent of pH over the range studied (pH 5–7; data not shown). Melting of the arabino (*A*) strand would be expected to be sensitive to pH because its association involves C^+·GC triads in which the hydrogen bonded arabinocytidine residues are protonated. The high temperature transition is assigned to melting of the hairpin duplexes, since it was also observed when a solution of duplex alone was heated under identical conditions. As can be seen from the melting curves shown in Figure 3, the *A* strand has a higher affinity for the DR duplex than the DD duplex (T_m 43 versus 34°C). Biphasic melting behavior was also observed for the control triplexes *D*·DD and *D*·DR, in agreement with the

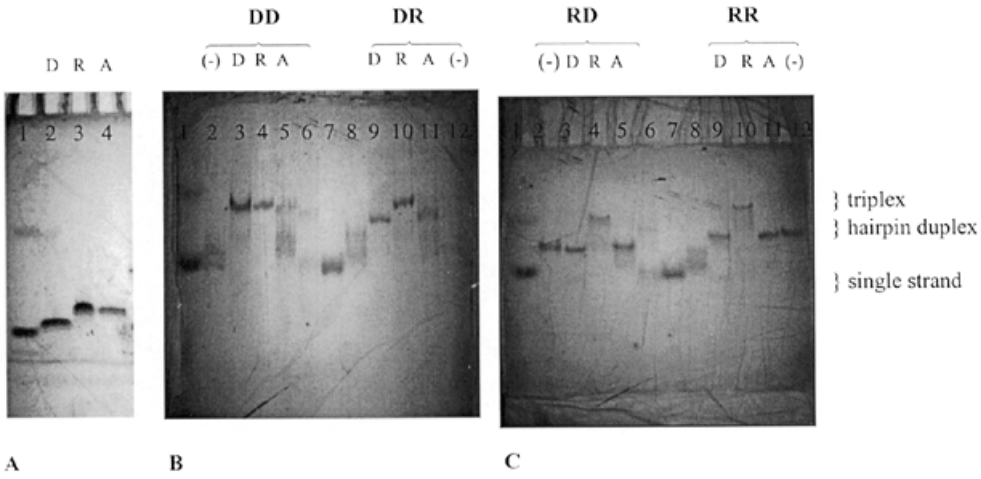

Figure 4. (**A**) Gel mobility shift assay of single strands under denaturing conditions; 7 M urea, 14% polyacrylamide, pH 8. (**B** and **C**) Gel mobility shift assay under non-denaturing conditions; 20% polyacrylamide, pH 5.0. Lane 1, marker dyes xylene cyanol (XC) and bromophenol blue (BPB). The DR complex is not clearly seen in lane 12, however, it moves faster than the complexes it forms (with a mobility very similar to the BPB dye).

results of Roberts and Crothers (Fig. 3; 17). The T_m for dissociation of *A* from DD and DR are ~2–8°C less than those for the corresponding triplexes formed by *D*. For mixtures *A* + RD and *A* + RR only the transition corresponding to duplex melting was observed, which exactly parallels what was observed for *D* + RD and *D* + RR mixtures (Table 1; 17–21). This is in clear contrast to the oligoribonucleotide (*R*), which formed stable triplexes with all DD, DR, RD and RR duplexes (17–21). In summary, these results show that *A* and *D* associate only with DD and DR, whereas *R* associates with all four duplexes.

Gel mobility shift detection of triplex formation

To confirm the above observations, triple-helix formation was monitored by non-denaturing gel electrophoresis. The results of such experiments are shown in Figure 4. When tested alone on a denaturing gel, *D*, *A* and *R* appeared as a single, well-defined band with the expected electrophoretic mobility (Fig. 4A). The situation is different under non-denaturing conditions, where *D* and *A* (but not R) form self-structures detectable by the presence of numerous bands of low mobility (Fig. 4B and C). The self-associating structures of *D* and other deoxycytidine-rich sequences have been described in detail (17,31) and are believed to be complexes in which the cytosines are base paired (C^+C). Consistent with this notion, the CD spectra of *A* and *D* (Fig. 5A) exhibited a positive band at ~282 nm and a negative band centered at ~260 nm, which is strongly indicative of C^+·C base pairs expected in *i*-motifs or C^+·C duplexes (32,33). The *D* strand (T_m 23°C, *H* 12%) appears to be more structured than the *A* strand (T_m 22°C, *H* 4%), as assessed by the amplitudes of the Cotton effects, gel mobility and thermal denaturation.

Strand *A* interacted with DD and DR, as evidenced by the appearance of a new band of reduced mobility (Fig. 4B). Not all *A* was shifted to triplexes under these conditions (A:duplex stoichiometry 1:1), as can be seen in the gel picture shown in Figure 4B. This is in contrast to the incubation of *D* with DD and DR which, under the same conditions, produced *D*·DD and *D*·DR in quantitative yields (Fig. 4B). The mobility of RD and RR was unaffected by incubation with either *A* or *D* (Fig. 4C), confirming the UV thermal melting results that triplexes *A*(or *D*)·RD and *A*(or *D*)·RR do not form under these conditions. Finally, incubation of *R* with any duplex gave rise to the expected triplexes with decreased mobilities (Fig. 4B and C).

Circular dichroism (CD)

As noted by Roberts and Crothers (17), the hairpin duplexes exhibited considerable differences in CD spectra (Fig. 5B). The CD spectrum of the DR hybrid is closer to that of the pure DD duplex, while the CD spectrum of RD resembles that of the pure RR duplex. The situation is different in the case of the triplexes, which exhibited appreciable spectral similarities (Fig. 5C–F). For example, the spectrum of *A*·DR is strikingly similar to that of *R*·DR, being only slightly different to the *D*·DR spectrum (Fig. 5D). The differences are mainly located in the region around 280 nm, where the *D*·DR (and *D*·DD) spectrum shows 'red-shifted' Cotton effects. These similarities are most likely the result of the conformation of the underlying duplex, e.g. DR, which dominates the CD spectra, rather than the three-dimensional arrangement (e.g. sugar puckering), of the constituent strands (see Discussion). The CD spectrum of a 1:1 mixture of *A* and RD or *A* and RR shows reduced band intensities and does not differ significantly from the calculated average of the spectra of A + RD or A + RR, consistent with a lack of association of these compounds.

DISCUSSION

The formation of triple-helices has become an area of great interest to chemists and biologists for their possible role in natural and artificial regulation of gene expression or for use in analytical, diagnostic or synthetic methods (6–8). Much work has been focused on the physical and chemical requirements for triplex formation, yet the precise conditions required are still not fully elucidated. Dissecting the relative contributions of all factors controlling triple helix formation will be pivotal when considering the use of modified oligonucleotides for *in vivo* applications where temperature, pH and ionic conditions are strictly con-

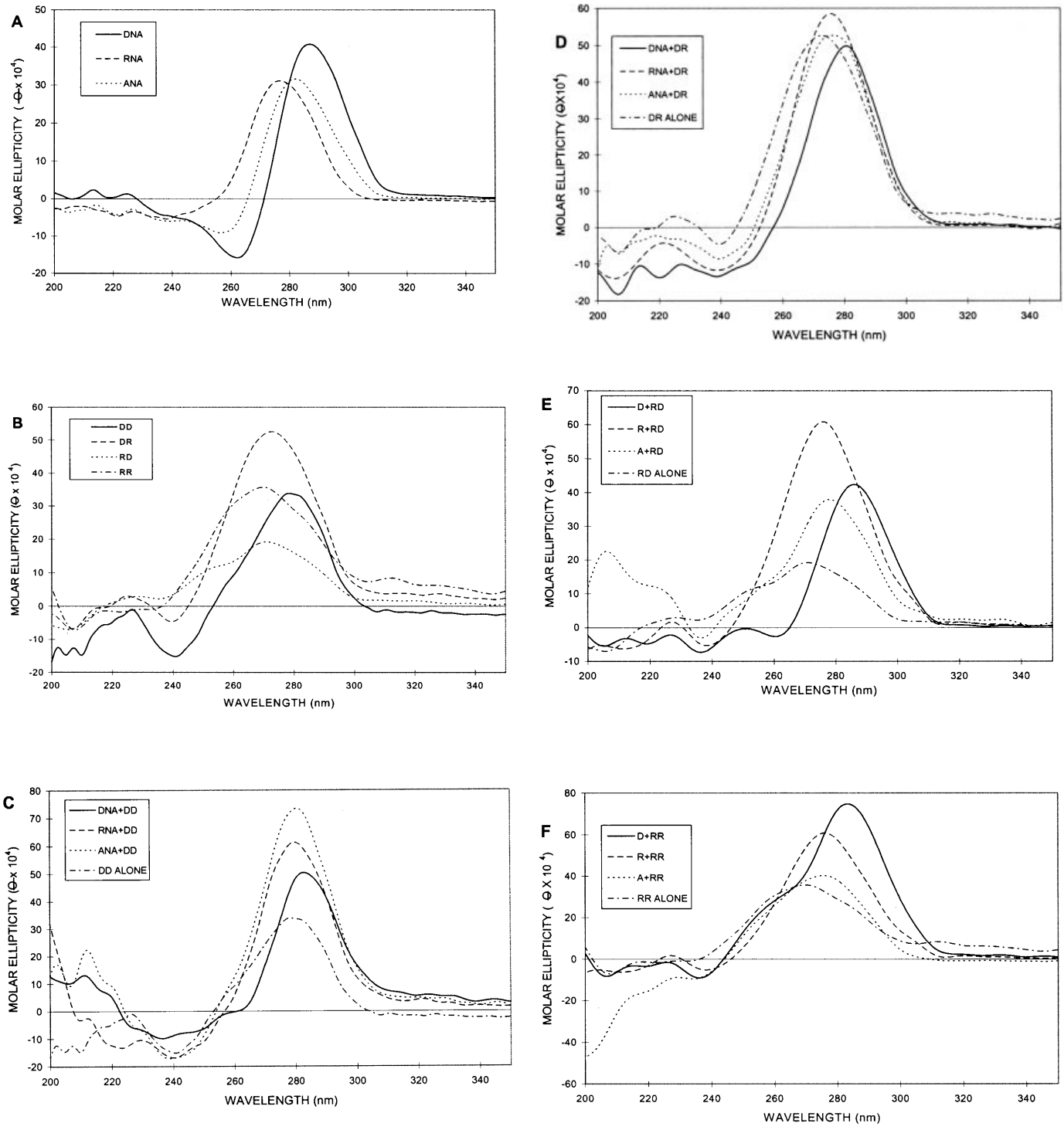

Figure 5. Circular dichroism (CD) of (**A**) single strands, (**B**) hairpin duplexes and (**C–F**) mixtures of hairpin + single strands as indicated. Concentration is 2 µM in each strand and the buffer is 100 mM sodium acetate, 1 mM EDTA (pH 5.5).

trolled. Roberts and Crothers (17) first described the sensitivity of triple helix stability to the backbone composition (DNA versus RNA). An RNA third strand was found to have strong effects on the stability of Py·PuPy or 'pyrimidine motif' triplexes. Subsequent studies led to the conclusion that conformational and steric differences in the ribose versus deoxyribose backbone, as a result of the 2′-OH group, may play a crucial role (18–21).

In order to gain a better understanding of the effect of sugar composition on triplex stability, we have investigated whether arabinonucleic acids (ANA or *A*) can be employed to recognize

pure duplex DNA, pure duplex RNA and RNA·DNA hybrids. The results presented above demonstrate that the pyrimidine motif does not accommodate oligoarabinonucleotides in triple helices with duplex RNA (RR) or hybrid RNA (Pur):DNA (Pyr) (RD). However, arabinopyrimidines can act as the third strand in recognition of duplex DNA (DD) and hybrid DNA (Pur):RNA (Pyr) (DR). The selectivity of ANA third strands for DD and DR duplexes, over RD and RR duplexes, exactly parallels that previously observed for DNA third strands (17–21). In contrast, RNA strands (the 2′-epimer of ANA strands) show a different behavior, forming stable triplexes with all four DD, DR, RD and RR duplexes. Comparison of the T_m data for the various triplexes revealed that those with an ANA third strand were thermally less stable than those with RNA strands, but similar to those with a DNA third strand.

Various reasons may be invoked to explain: (i) the contrasting hybridization behavior of ANA and RNA third strands; (ii) the similar binding characteristics of ANA and DNA strands. A possible interpretation for (i) is that in the case of RNA, the stereochemistry of the sugar favors formation of short contacts between the 2′-OH groups of the third strand and the purine strand phosphates, as predicted by the computational model (19), whereas for the 2′-epimeric ANA strands such a mechanism may not be possible. Another possible explanation, which reconciles both (i) and (ii) above, is that arabinonucleotides mimic deoxyribonucleotide rather than ribonucleotide conformations. The sugars in RNA adopt primarily the C3′-*endo* pucker, regardless of whether the RNA is found in single-stranded, double- or triple-helical forms. Such conformation is governed by anomeric effects of the C1′ and C4′ substituents with the ring oxygen and/or stereochemical requirements of complex formation (34–36). This situation differs from DNA, where an O3′ gauche effect to O4′ favors the C2′-*endo* pucker (34–36), particularly in aqueous solution (Fig. 6). For example, Dagneaux *et al*. showed that the sugars of DNA triplexes (T·AT) assume the C2′-*endo* conformation, while triplexes containing a ribo third strand have mainly C3′-*endo*-type, e.g. R(C3′-*endo*)·D(C3′-*endo*):D(C2′-*endo*) and R(C3′-*endo*)·R(C3′-*endo*):R(C3′-*endo*) (37). Arabinonucleotides are expected to mimic deoxyribonucleotides since a combination of O2′→O4′ and O3′→O4′ gauche effects would stabilize the C2′-*endo* geometry (Fig. 6).

Although we have not yet determined the conformation of arabinonucleotide strands in a double- or triple-helix, analysis of several lines of evidence points to the contention that ANA mimics DNA, not RNA. (i) In a recent NMR study, a DNA duplex containing two 2′-*O*-methyl-β-D-araT insertions was found to adopt a normal B-type DNA helix, with the arabinonucleosides found in the C2′-*endo* sugar conformation (38). (ii) X-ray crystallographic studies on araC nucleosides and on DNA duplexes containing araC indicated that the arabinose sugar possessed either the C1′-*exo* or the C2′-*endo* conformation typical of B-type DNA (39–41). (iii) Introduction of an araC residue into the Drew–Dickerson duplex did not result in gross distortion of a right-handed, B-type DNA double helix. Interestingly, in this case the arabinose sugar was closer to the C3′-*endo* than the C2′-*endo* domain (42). (iv) Oligodeoxyribocytidine and oligoarabinocytidine but not oligoribocytidine strands can fold into C-tetrads or *i*-motifs (27). (v) Perhaps the most definite is the finding that the CD spectra of ANA·RNA duplexes of mixed base composition are virtually identical to those of DNA·RNA duplexes (A-like hybrids) and different from those of the pure

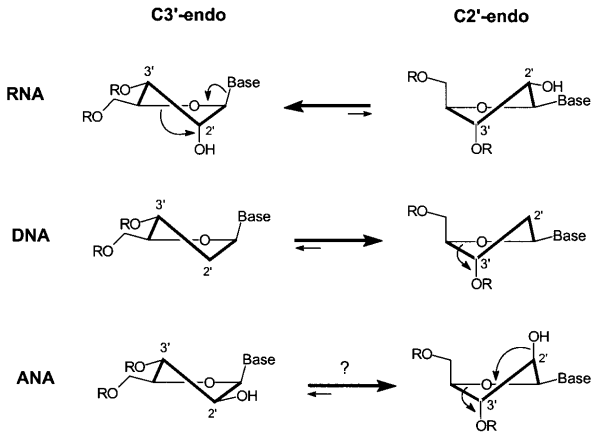

Figure 6. Sugar puckering conformational equilibrium for RNA, DNA and ANA strands. Sugars of DNA triplexes assume the C2′-*endo* conformation, while triplexes containing an RNA third strand have mainly the C3′-*endo* conformation (34,37). ANA strands are expected to mimic DNA conformation since a combination of O2′→O4′ and O3′→O4′ gauche effects would stabilize the C2′-*endo* geometry. The light arrowheads associated with each favored confomer indicate stabilizing stereoelectronic effects (gauche and anomeric effects).

RNA duplexes (Noronha and Damha, unpublished results). It is thus tempting to speculate that oligonucleotide analogs with C3′-*endo*-like sugars (with or without a 2′-OH group) will recognize all four possible dispositions of DNA and/or RNA strands in a Watson–Crick duplex, whereas those adopting the C2′-*endo* pucker will recognize only DD and DR duplexes. The finding that 2′,5′-linked RNA (C2′-*endo*) binds only to DD and DR, but not RD and RR (A.Noronha and M.J.Damha, unpublished results), and the fact that 2′,5′-linked ssDNA (C3′-*endo*) binds to RR but not DD (43), support this view.

In summary, the results of our experiments are in agreement with previous studies of others and show that triplex formation is sensitive to backbone composition. Our results show, for the first time, that arabinonucleic acids are able to recognize double helical complexes, demonstrating that the stereochemistry of the 2′-OH groups of a triplex-forming RNA strand can be inverted, but not without affecting the hybridization properties of such strands and the stability of the complexes formed. Such an understanding can be applied to the design of sequence-selective oligonucleotides which interact with double-stranded nucleic acids and emphasizes the role of the 2′-OH as a general recognition and binding determinant of RNA. Finally, our results are likely to stimulate experimental work on arabinose derivatives in laboratories concerned with targeting DNA sequences *in vivo*, since ANA oligomers are more resistant to nuclease degradation relative to natural deoxyribose (DNA) oligomers (25; unpublished results).

ACKNOWLEDGEMENTS

We acknowledge the Natural Science and Engineering Council of Canada (NSERC) and Les Fonds pour la Formation de Chercheurs et l'Aide a la Recherche (FCAR) for support of this work. We thank C.Wilds for assistance in the preparation of this manuscript.

REFERENCES

1 Sanghvi,Y.S. and Cook,P.D. (1994) In Sanghvi,Y.S. and Cook,P.D. (eds), *Carbohydrate Modifications in Antisense Research*, ACS Symposium Series. American Chemical Society, Washington, DC, Vol. 580, pp. 1–23.
2 Various (1997) *Nature Biotechnol*., **15**, 519–524.
3 Letsinger,R.L. and Lunsford,W.B., (1976) *J. Am. Chem. Soc*., **98**, 3655–3661.
4 Beaucage,S. and Caruthers,M.H. (1981) *Tetrahedron Lett*., **22**, 1859–1862.
5 Alvaredo-Urbina,G., Sathe,G.M., Liu,W.-C., Gillen,M.F., Duck,P.D., Bender,R. and Ogilvie,K.K. (1981) *Science*, **214**, 270–274.
6 Maher,L.J. (1992) *BioEssays*, **14**, 807–815.
7 Mirkin,S.M. (1995) *Annu. Rev. Biochem*., **64**, 65–95.
8 Neidle,S. (1997) *Anti-Cancer Drug Design*, **12**, 433–442.
9 Giovannangeli,C., Perrouault,L., Escude,C., Thuong,N. and Helene,C. (1996) *Biochemistry*, **35**, 10539–10548.
10 Uddin,A.H., Piunno,P.A.E., Hudson,R.H.E., Damha,M.J. and Krull,U.J. (1997) *Nucleic Acids Res*. **25**, 4139–4146.
11 Strobel,S.A., Doucettestamm,L.A., Riba,L., Housman,D.E. and Dervan,P.B. (1991) *Science*, **254**, 1639–1642.
12 Ito,T., Smith,C.L. and Cantor,C.R. (1992) *Proc. Natl. Acad. Sci. USA*, **89**, 495–498.
13 Wang,S.H., Friedman,A.E. and Kool,E.T. (1995) *Biochemistry*, **34**, 9774–9784.
14 Felsenfeld,G., Davies,D.R. and Rich,A.J. (1957) *J. Am. Chem. Soc*., **79**, 2023–2024.
15 Moser,H.E. and Dervan,P.B. (1987) *Science*, **238**, 645–650.
16 Le Doan,T., Perrouault,L., Praseuth,D., Habhoub,N., Decout,J.L., Thoung,N.T., Lhomme,J. and Helene,C. (1987) *Nucleic Acids Res*., **15**, 7749–7760.
17 Roberts,R.W. and Crothers,D.M. (1992) *Science*, **258**, 1463–1466.
18 Han,H. and Dervan,P.B. (1993) *Proc. Natl. Acad. Sci. USA*, **90**, 3806–3810.
19 Escude,C., Francois,J.-C., Sun,J., Gunther,O., Sprinzl,M., Garestier,T. and Helene,C. (1993) *Nucleic Acids Res*., **21**, 5547–5553.
20 Han,H. and Dervan,P.B. (1994) *Nucleic Acids Res*., **22**, 2837–2844.
21 Wang,S. and Kool,E.T. (1994) *Nucleic Acids Res*., **22**, 2326–2333.
22 Semerad,C.L. and Maher,L.J. (1994) *Nucleic Acids Res*., **24**, 5321–5325.
23 Skoog,J.U. and Maher,J.L. (1993) *Nucleic Acids Res*., **21**, 2131–2138.
24 Shimizu,M., Konishi,A., Shimada,Y., Inoue,H. and Ohtsuka,E. (1992) *FEBS Lett*., **302**, 155–158.
25 Giannaris,P.A. and Damha,M.J. (1994) *Can. J. Chem.*, **72**, 909–918.
26 Noronha,A. and Damha,M.J. (1997) *J. Biomol. Struct. Dyn*., **14**, 805–806.
27 Robidoux,S. and Damha,M.J. (1997) *J. Biomol. Struct. Dyn.*, **15**, 529–535.
28 Damha,M.J., Giannaris,P.A. and Zabarylo,S.V. (1990) *Nucleic Acids Res*., **18**, 3813–3821.
29 Damha,M.J. and Ogilvie,K.K. (1993) In Agrawal,S. (ed.), *Methods in Molecular Biology—Protocols for Oligonucleotides and Analogs.* Humana Press, Totowa, NJ, Vol. 20, pp. 81–114.
30 Puglisi,J.D. and Tinoco,I.,Jr (1989) In Dahlberg,J.E. and Abelson,J.N. (eds), *Methods in Enzymology.* Academic Press, New York, NY, Vol. 180, pp. 304–325.
31 Singh,S., Patel,P.K. and Hosur,R.V. (1997) *Biochemistry*, **36**, 13214–13222.
32 Manzini,G., Yathindra,N. and Xodo,L.E. (1994) *Nucleic Acids Res*., **22**, 4634–4640.
33 Kanehara,H., Mizuguchi,M., Tajima,K., Kanaori,K. and Makino,K. (1997) *Biochemistry*, **36**, 1790–1797.
34 Saenger,W. (1984) *Principles of Nucleic Acids Structure*. Springer-Verlag, New York, NY.
35 Plavec,J., Thibaudeau,C. and Chattopadhyaya,J. (1994) *J. Am. Chem. Soc*., **116**, 6558–6560.
36 Thibaudeau,C., Plavec,J. and Chattopadhyaya,J. (1994) *J. Am. Chem. Soc*., **116**, 8033–8037.
37 Dagneaux,C., Liquier,J. and Taillandier,E. (1995) *Biochemistry*, **34**, 16618–16623.
38 Gotfredsen,C.H., Spielmann,P. Wengel,J. and Jacobsen,J.P. (1996) *Bioconjugate Chem*., **7**, 680–688.
39 Chwang,A.K. and Sundaralingam,M. (1973) *Nature*, **243**, 78–79.
40 Teng,M.-K., Liaw,Y.-C., van der Marel,G.A., van der Marel,G.A., van Boom,J.H. and Wang,A.H.-J. (1989) *Biochemistry*, **28**, 4923–4928.
41 Gao,Y.-G., van der Marel,G.A., van Boom,J.H. and Wang,A.H.-J. (1991) *Biochemistry*, **30**, 9922–9931.
42 Schweitzer,B.I., Mikita,T., Kellogg,G.W., Gardner,K.H. and Beardsley,G.P. (1994) *Biochemistry*, **33**, 11460–11475.
43 Singh,R.K., Takai,K. and Takanu,H. (1996) *Nucleic Acids Symp. Series*, **35**, 119–120.